

UNCLASSIFIED

AD NUMBER

ADB006666

LIMITATION CHANGES

TO:

Approved for public release; distribution is unlimited.

FROM:

Distribution authorized to U.S. Gov't. agencies only; Test and Evaluation; 10 APR 1975. Other requests shall be referred to Air Force Cambridge Research Labs., Hanscom AFB, MA.

AUTHORITY

AFCRL ltr 6 Nov 1980

THIS PAGE IS UNCLASSIFIED

**THIS REPORT HAS BEEN DELIMITED  
AND CLEARED FOR PUBLIC RELEASE  
UNDER DOD DIRECTIVE 5200.20 AND  
NO RESTRICTIONS ARE IMPOSED UPON  
ITS USE AND DISCLOSURE.**

**DISTRIBUTION STATEMENT A**

**APPROVED FOR PUBLIC RELEASE,  
DISTRIBUTION UNLIMITED.**

L

ADB006666

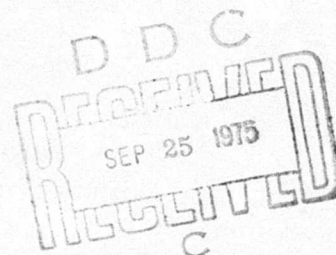
AFCRL-TR-75-0207  
AIR FORCE SURVEYS IN GEOPHYSICS, NO. 308



# Final Report of STM-8W Weather Documentation AFCRL/Minuteman Report No. 3

JAMES I. METCALF, Capt, USAF  
ARNOLD A. BARNES Jr.  
MICHAEL J. KRAUS

11 April 1975



Distribution limited to U.S. Government agencies only;  
(Test & Evaluation; Test and Evaluation of Military  
Systems/Equipment); (10 April 1975). Other requests  
for this document must be referred to AFCRL (LYW),  
Hanscom AFB, Massachusetts 01731

METEOROLOGY LABORATORY PROJECT 133B  
**AIR FORCE CAMBRIDGE RESEARCH LABORATORIES**  
HANSCOM AFB, MASSACHUSETTS 01731

**AIR FORCE SYSTEMS COMMAND, USAF**



Qualified requestors may obtain additional copies from the  
Defense Documentation Center.





**Figure 4.** Montage of Photographs From WB-57F Downward-Looking Camera. Flight is at 18 km altitude at a true heading of  $236^{\circ}$  along the reentry corridor at 0439-0445Z. No high clouds are visible. Patches of low or middle cloud are visible to the southeast (lower left) and to the northwest (upper right) beyond Roi-Namur Island. Reentry corridor is clear except for low-level cumulus. Islands of Kwajalein Atoll appear in the upper part of the figure

AFCRL-TR-75-0207  
Air Force Surveys in Geophysics, No. 308

Final Report of STM-8W Weather Documentation  
AFCRL/Minuteman Report No. 3

James I. Metcalf, Capt, USAF  
Arnold A. Barnes, Jr.  
Michael J. Kraus

#### ERRATA

Upon printing, Figure 4 on page 11 was inadvertently reversed.  
Please replace it with the correct figure furnished on the other side  
of this notice.

Meteorology Laboratory  
Air Force Cambridge Research Laboratories  
Hanscom AFB, Massachusetts 01731

Project 133B

Air Force Systems Command, USAF

Unclassified

SECURITY CLASSIFICATION OF THIS PAGE (When Data Entered)

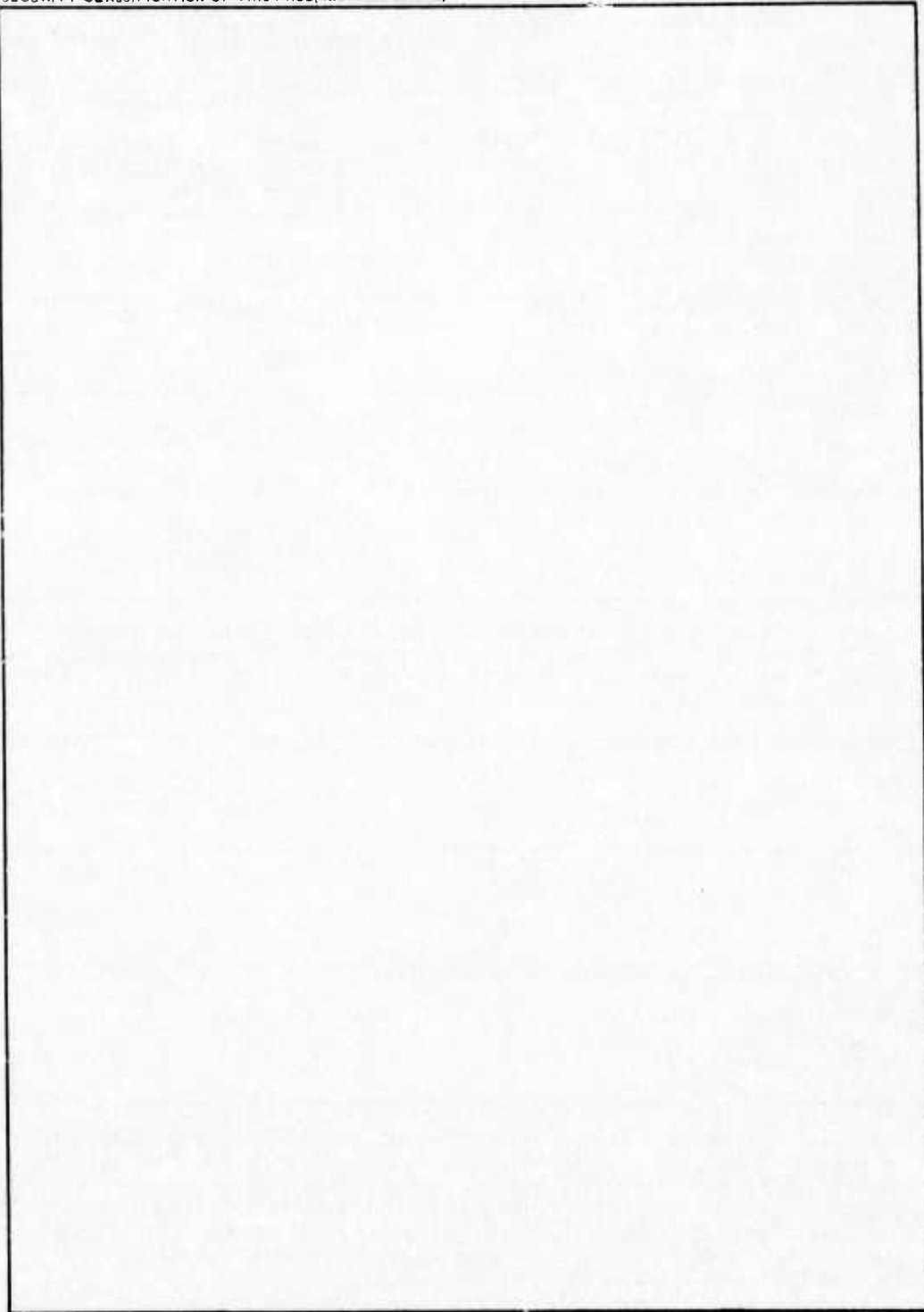
REPORT DOCUMENTATION PAGE		READ INSTRUCTIONS BEFORE COMPLETING FORM
1. REPORT NUMBER AFCRL-TR-75-0207	2. GOVT ACCESSION NO.	3. RECIPIENT'S CATALOG NUMBER
4. TITLE (and Subtitle) FINAL REPORT OF STM-8W WEATHER DOCUMENTATION AFCRL/Minuteman Report No. 3		5. TYPE OF REPORT & PERIOD COVERED Scientific. Final.
		6. PERFORMING ORG. REPORT NUMBER AFSG No. 308
7. AUTHOR(s) James I. Metcalf, Capt, USAF Arnold A. Barnes, Jr. Michael J. Kraus		8. CONTRACT OR GRANT NUMBER(s)
9. PERFORMING ORGANIZATION NAME AND ADDRESS Air Force Cambridge Research Laboratories (LYW) Hanscom AFB Bedford, Massachusetts 01731		10. PROGRAM ELEMENT, PROJECT, TASK AREA & WORK UNIT NUMBERS 133B0001
11. CONTROLLING OFFICE NAME AND ADDRESS Air Force Cambridge Research Laboratories (LYW) Hanscom AFB Bedford, Massachusetts 01731		12. REPORT DATE 11 April 1975
14. MONITORING AGENCY NAME & ADDRESS (if different from Controlling Office)		13. NUMBER OF PAGES 34
		15. SECURITY CLASS. (of this report) Unclassified
		15a. DECLASSIFICATION/DOWNGRADING SCHEDULE
16. DISTRIBUTION STATEMENT (of this Report) Distribution limited to U. S. Government agencies only; (Test & Evaluation; Test and Evaluation of Military Systems/Equipment); (10 April 1975). Other requests for this document must be referred to AFCRL (LYW), Hanscom AFB, Massachusetts 01731.		
17. DISTRIBUTION STATEMENT (of the abstract entered in Block 20, if different from Report)		
18. SUPPLEMENTARY NOTES		
19. KEY WORDS (Continue on reverse side if necessary and identify by block number) Minuteman Aircraft weather measurement Radar weather measurement Tropical cirrus cloud Water content profiles		
20. ABSTRACT (Continue on reverse side if necessary and identify by block number) Reentry weather encountered by Minuteman test STM-8W is described. Documentation was accomplished by WB-57F aircraft, by satellite, by radar, and by lidar. A thin cloud layer was present at about 8.5 km with ice water content about $0.003 \text{ gm m}^{-3}$ , and one at 5.5 km had about $0.002 \text{ gm m}^{-3}$ . Low-level cumulus clouds were observed below 3 km on two of the trajec- tories. Data from all sources are presented, and operational problems of the weather documentation plan are discussed.		

Unclassified

SECURITY CLASSIFICATION OF THIS PAGE (When Data Entered)

Unclassified

SECURITY CLASSIFICATION OF THIS PAGE(When Data Entered)



Unclassified

SECURITY CLASSIFICATION OF THIS PAGE(When Data Entered)



## Preface

AFCRL participation in the Minuteman Natural Hazards Program, which began with the planning and field support of the PVM-3 test,<sup>1</sup> continued with the STM-8W test in December 1973. Improvements in the data acquisition plan based on the earlier experience in the field were incorporated into this mission support. The field support included representatives of SAMSO/MN; SAMTEC/WE; 9th Weather Reconnaissance Wing (58th Weather Reconnaissance Squadron); 6th Weather Wing; AFCRL Meteorology Laboratory; TRW Systems Group; Meteorology Research, Inc.; Edgerton, Germeshausen, and Grier, Inc.; Particle Measuring Systems, Inc.; and Stanford Research Institute. TRW was responsible for the overall planning and operation of the test.<sup>2</sup> The roles of the other organizations are described in this report. MRI and SRI in particular were responsible for the operation of the aircraft instrumentation and the lidar, respectively, and readers interested in more details of their equipment or data than are presented below are referred to their final reports.<sup>3,4</sup>

1. Metcalf, J.I., Barnes, A.A., Jr., and Kraus, M.J. (1975b) Final Report of PVM-4 and PVM-3 Weather Documentation, AFCRL-TR-75-0097, Air Force Cambridge Research Laboratories, Hanscom AFB, MA.
2. Wilmot, R.A., Cisneros, C.E., and Guiberson, F.L. (1974) High cloud measurements applicable to ballistic missile systems testing, 6th Conf. Aerosp. and Aeronaut. Meteor., Am. Meteor. Soc., 194-199.
3. Jahnsen, L.J., and Heymsfield, A.J. (1974) STM-8W Mission WB-57F Instrumentation and Cloud Particle Measurements, MRI 74 FR-1189, Meteorology Research, Inc., Altadena, CA.
4. Uthe, E.E., Allen, R.J., and Russell, P.B. (1974) Light Detection and Ranging (LIDAR) Support for STM-8W and PVM-5 Reentry Operations, SRI Project 2859, Stanford Research Institute, Menlo Park, CA.

## Preface

Reports in the AFCRL/Minuteman Series are as follows:

No. 1 (23 Dec 1974) Aircraft and Radar Weather Data Analysis for PVM-5  
(AFCRL-TR-74-0627);

No. 2 (19 Feb 1975) Final Report of PVM-4 and PVM-3 Weather Documentation  
(AFCRL-TR-75-0097).

## Contents

1. INTRODUCTION	7
2. WEATHER DESCRIPTION	9
3. WB-57F WEATHER OBSERVATIONS	16
4. ALCOR WEATHER OBSERVATIONS	21
5. SUMMARY AND CONCLUSIONS	29
REFERENCES	31
SYMBOLS	33

## Illustrations

1. Kwajalein Atoll, Showing the Islands Occupied By the Facilities of Kwajalein Missile Range	8
2. DMSP (DAPP) Satellite Visual Data for 22 Dec 1973, 0114Z	9
3. DMSP (DAPP) Satellite Infrared Data for 22 Dec 1973, 0846Z	10
4. Montage of Photographs From WB-57F Downward-Looking Camera	11
5. WSR-57 PPI at 0603Z, 22 Dec 1973	13
6. WSR-57 PPI at 0822Z, 22 Dec 1973	14



## Illustrations

7a. Sounding From Kwajalein at 0830Z, 22 Dec 1973	15
7b. Sounding From Roi-Namur at 0840Z, 22 Dec 1973	15
8. Instrumentation Pod on Right Wing of WB-57F Aircraft	18
9. Instrumentation Pod on Left Wing of WB-57F Aircraft	18
10. Flight Pattern for WB-57F Cloud Sampling	19
11. Deviations of the WB-57F Aircraft From Nominal Flight Paths	20
12. Correlations of $Z'$ and M Derived From WB-57F Data at Kwajalein	21
13. Radar Weather Data Flow Diagram	23
14. ALCOR RHI Scans During Pre-mission Aircraft Operations	25
15a. ALCOR Scan of STM-8W RV1 Trajectory at 0828Z, 22 Dec 73	26
15b. ALCOR Scan of STM-8W RV1 Trajectory at 0838Z, 22 Dec 73	26
16a. ALCOR Scan of STM-8W RV2 Trajectory at 0836Z, 22 Dec 73	27
16b. ALCOR Scan of STM-8W RV2 Trajectory at 0839Z, 22 Dec 73	27
17. Approximate Minimum Detectable Ice Water Content on STM-8W Trajectories	28
18. Reflectivity Profile Observed on ALCOR Vertical Scan at 0837Z, 22 Dec 73	29

## Tables

1. Lidar Data Summary, December 1973	12
2. WB-57F Operations at Kwajalein, December 1973	17
3. ALCOR Weather Support for STM-8W, 22 Dec 1973	22

## Final Report of STM-8W Weather Documentation AFCRL/Minuteman Report No. 3

### 1. INTRODUCTION

The Minuteman STM-8W test was launched on 22 December 1973, with reentry near Kwajalein Atoll at 0834Z. This report describes the weather data acquisition plan and presents our best determination of the water content profile encountered by the reentry vehicles. Data from various meteorological sensors are presented to provide further details on the local weather, both on the macro-scale of clouds and weather systems and on the microscale of particle shapes and sizes.

Descriptions of each of the sensors are included with the presentations of data in the following sections. The locations of the various supporting facilities are shown in Figure 1. The NWS rawinsonde and weather radar facilities and the DMSP (formerly DAPP) satellite van operated by the 6th Weather Wing from McClellan AFB were located on Kwajalein Island. The lidar operated by SRI was located on Gellinam Island, close to the reentry corridor. The Lincoln Laboratory radars, located at KREMS on Roi-Namur Island, were used to obtain weather data on the reentry trajectories. NWS rawinsonde facilities at Roi-Namur Island were used for soundings in conjunction with the mission, in addition to the soundings from Kwajalein. Two WB-57F aircraft operated by the 58th Weather Reconnaissance Squadron from Kirtland AFB were based at Kwajalein for the STM-8W test support.

(Received for publication 10 April 1975)

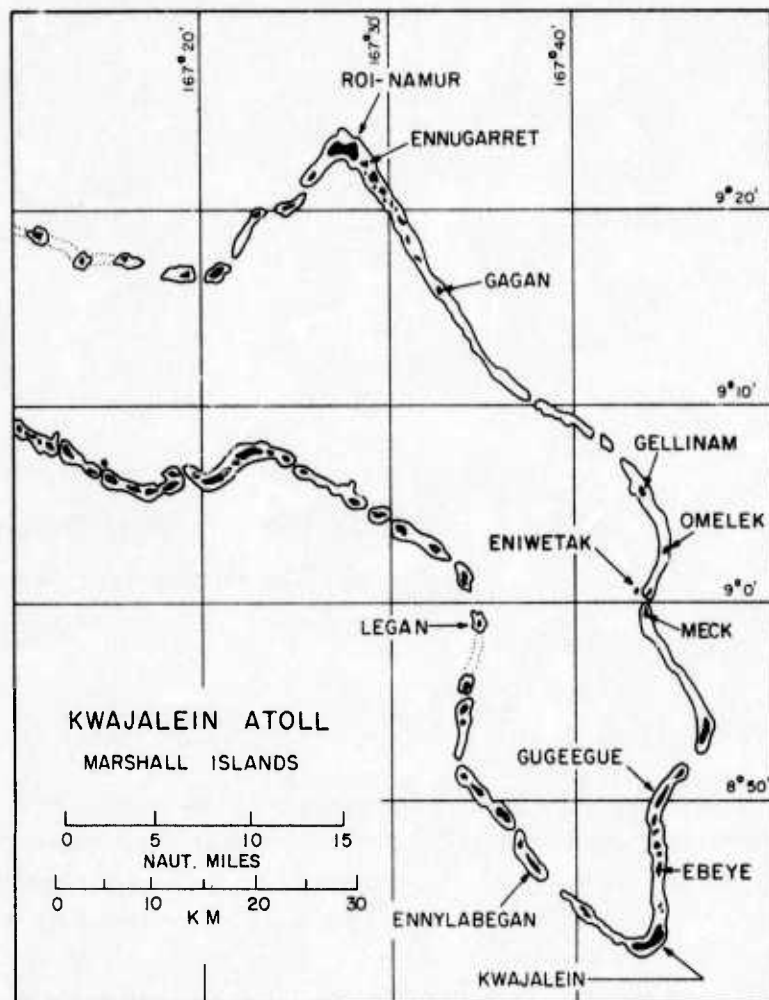


Figure 1. Kwajalein Atoll, Showing the Islands Occupied by the Facilities of Kwajalein Missile Range. Range Operations Control Center, aircraft support facilities, NWS radars, and MPS-36 radars are at Kwajalein Island. Lincoln Laboratory radars and NWS rawinsonde site are at Roi Namur Island

Execution of the weather data acquisition plan and on-site evaluation of the data were the responsibilities of the Mission Weather Team, which was at Kwajalein during the period 12-22 December 1973. The Weather Team included representatives of AFCRL,<sup>†</sup> SAMSO, SAMTEC, TRW, and MRI at the ROCC during operations, and two AFCRL radar meteorologists<sup>‡</sup> at KREMS.

<sup>†</sup> L. D. Nelson

<sup>‡</sup> A. A. Barnes, Jr., and Capt J. I. Metcalf

The weather criterion for the mission was "minimum weather", defined as optically translucent clouds no greater than 2000 ft (610 m) thick, to be determined by vertical visual observation from an aircraft. The analysis shows that this objective was met. The lidar observed no clouds in the reentry corridor or toward the zenith within 2 hr before and after the reentry. Radar weather scans of the RV1 trajectory revealed a thin cirrus layer near 8.5 km with water content about  $0.003 \text{ gm m}^{-3}$ , and a layer at about 5.5 km with water content about  $0.002 \text{ gm m}^{-3}$ . Clouds were observed below 3.3 km on the RV1 and RV2 trajectories, but it is probable that the 8.5-km layer extended across all three trajectories.

## 2. WEATHER DESCRIPTION

The DMSP visual photograph taken at 0114Z (Figure 2) showed no detectable cirrus clouds in the Kwajalein area or to the east to a range of 350 km. A group

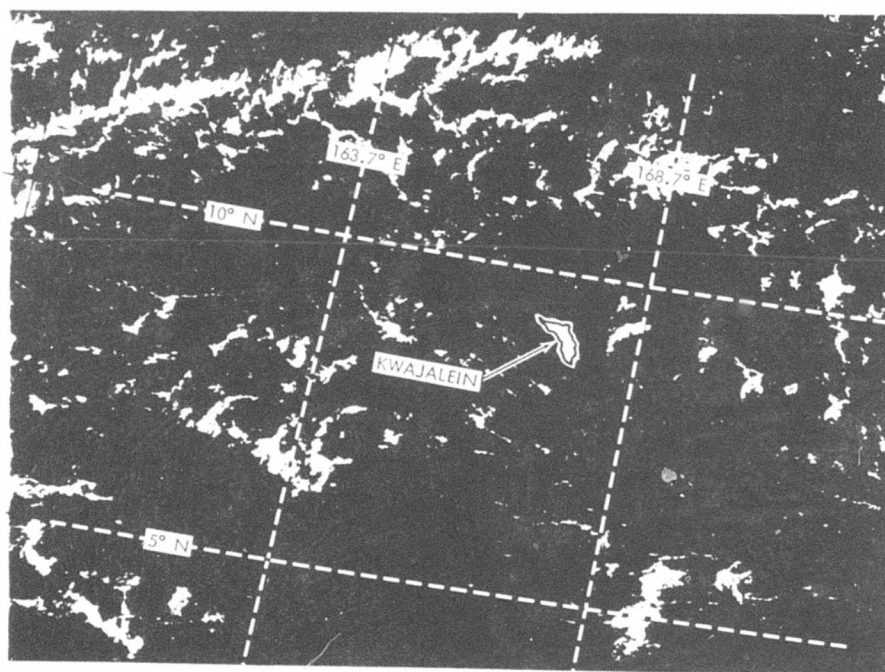


Figure 2. DMSP (DAPP) Satellite Visual Data for 22 Dec 1973, 0114Z. No cirrus clouds are visible within about 350 km east of Kwajalein or 180 km west. The weather about 50 to 100 km east of the atoll, near  $168.5^\circ \text{E}$ , is a group of cumulus clouds which passed over Kwajalein about 0215Z



of towering cumulus clouds located about 50 to 100 km east of the atoll at that time passed over Kwajalein about 0215Z. The DMSP infrared photograph taken at 0846Z (Figure 3) showed no cloud masses greater than 3.5 km in diameter (the photo resolution) in the target area. A group of showers discernable about 45 km northwest of Kwajalein was probably the same group which passed through the target area about 15 min before impact. A large thunderstorm was located about 150 km east of Kwajalein, but northeasterly winds near the storm top carried any cirrus blowoff to the south of the reentry corridor.

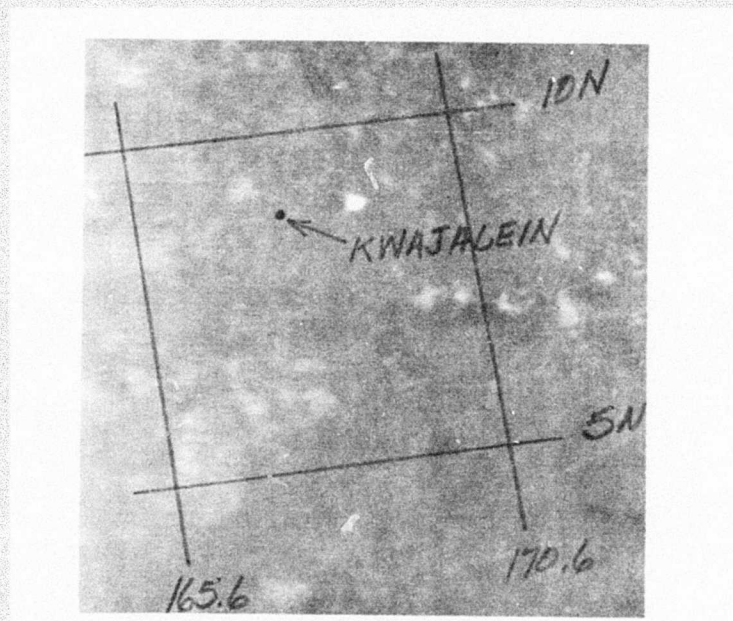
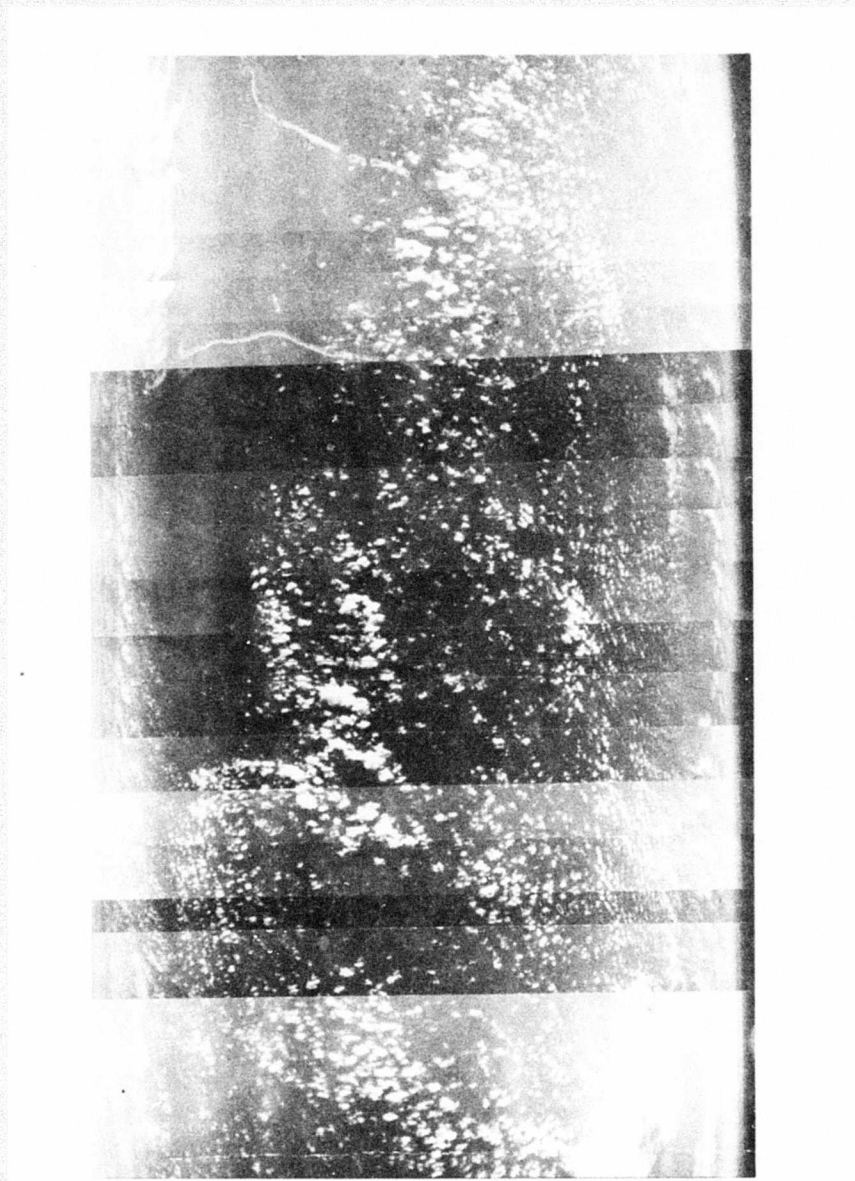


Figure 3. DMSP (DAPP) Satellite Infrared Data for 22 Dec 1973, 0846Z. No cloud masses greater than 3.5 km in diameter (the photo resolution) are in the target area. The clouds approximately 45 km northwest of Kwajalein are probably the remnants of the line of showers which passed through the target area about 15 min before RV impact. A thunderstorm is located about 150 km east of Kwajalein, but the northeasterly winds would have carried any cirrus blowoff to the south of the reentry corridor

The WB-57F aircraft made a photo run at 18 km (60 kft) over the reentry corridor at 0439-0445Z. Photographs from the downward-looking panoramic camera (Figure 4) showed only low-level fair weather cumulus clouds in the



**Figure 4. Montage of Photographs From WB-57F Downward-Looking Camera. Flight is at 18 km altitude at a true heading of 236° along the reentry corridor at 0439-0445Z. No high clouds are visible. Patches of low or middle cloud are visible to the southeast (lower left) and to the northwest (upper right) beyond Roi-Namur Island. Reentry corridor is clear except for low-level cumulus. Islands of Kwajalein Atoll appear in the upper part of the figure**



reentry area and a few patches of stratocumulus clouds toward the horizons. The forward-looking camera revealed some high cirrus during the cloud sampling operations, and persistent contrails. The thin, so-called "invisible", cirrus clouds near the tropopause are not uncommon in the tropics. Depending on the position of the sun and the angle of view, it may be observed from the ground or from an aircraft. In this and other cases the PMS data indicated ice water content less than  $0.001 \text{ gm m}^{-3}$  in the vicinity of these layers.

The SRI Mark IX lidar<sup>4</sup> was at KMR from 12 to 22 December 1973. The Mark IX system uses a pulsed ruby laser at a wavelength of  $6943 \text{ \AA}$ . Backscattered signal intensity, which depends primarily on the integrated cross-sectional area of the cloud or aerosol particles, was measured and provided a means of determining ice water content or density. (Signal attenuation may limit the accuracy of the lidar measurements in thick clouds.) A summary of the lidar operations is presented in Table 1. On STM-8W mission day, the lidar operated from 2238Z (21 Dec) to 0922Z (22 Dec) with a maximum range of 20 km for vertical scans. Elevation scans taken in the reentry corridor at  $50^\circ$  azimuth from Gellinam Island were made at 0831 to 0841Z, close to the time of reentry. A cloud layer about 19-km altitude persisted for over 2 hr during the late afternoon, but was not detected after 0550Z. The lidar detected no clouds during the reentry or for 45 min after impact.

Table 1. Lidar Data Summary, December 1973

Date (1973)	Time (GMT)	Number of Shots	Rate (pulses/Minute)	Remarks
16 Dec	0041-0113	160	5	Lidar check-out
17 Dec	2117-0355 (18 Dec)	1,196	4	Digital data recorded, 19 km cirrus
20 Dec	0246-0318	160	5	Work on digital system, 18 km cirrus
20 Dec	2115-2155	160	4	Cloud layers to 15 km
	2308-2348	160	4	Dense low clouds
21 Dec	0108-0342	420	4	
21 Dec	2238-0829 (22 Dec)	2,346	4	STM-8W mission day, 19 km cirrus from 0328 to 0550Z
22 Dec	0831-0841	210	20	Angular scans in the reentry corridor Azimuth = $50^\circ$ Elevation = $35^\circ$ to $70^\circ$
	0842-0922	160	4	No high clouds observed during reentry



The NWS 10-cm WSR-57 weather radar at Kwajalein can detect precipitation but cannot detect non-precipitating clouds. A radar scan at 0603Z (Figure 5) near the end of the WB-57F operations showed only scattered convective cells except for a line of showers approaching from the east. These passed over the target

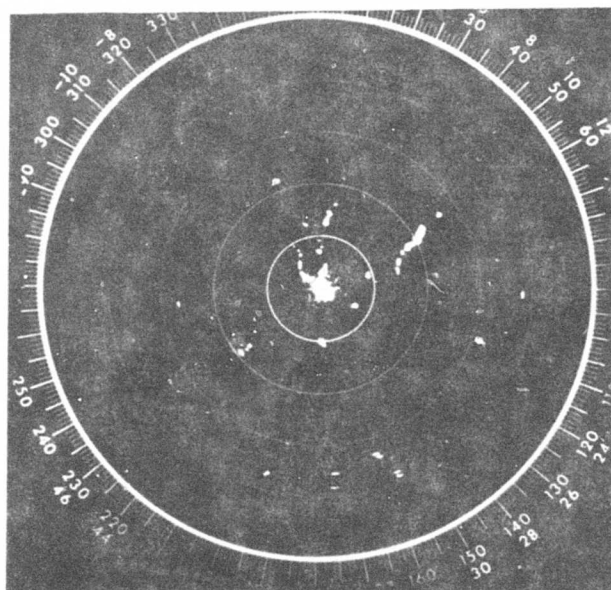


Figure 5. WSR-57 PPI at 0603Z, 22 Dec 1973. Elevation angle is  $0^\circ$  and range markers are at 25 n.m. (46.3 km) intervals out to 125 n.m. (231.5 km). Ground echoes from the atoll islands appear to the north and northwest as far as about 40 km. Isolated showers are detectable in all directions. A line of showers about 68 km east of Kwajalein passed over the atoll just before the reentry

area, as noted above, and were located over the northwestern part of the atoll at 0822Z, as can be seen in Figure 6. These were moving toward  $260^\circ$  at a speed of about  $13 \text{ m sec}^{-1}$ , and at the time of impact the maximum tops were near 4.6 km (15 kft). At launch time most of the cell tops had been at 6 to 7.5 km (20 to 25 kft) with the maximum top at 10.7 km (35 kft) as observed by the WSR-57.

The Kwajalein and Roi-Namur radiosondes released close to the time of impact are shown in Figure 7. Winds were from the northeast quadrant from the surface to the tropopause near 18 km. Both soundings were moist to about 2.5 km and showed relatively moist layers up to about 13 km, which is consistent

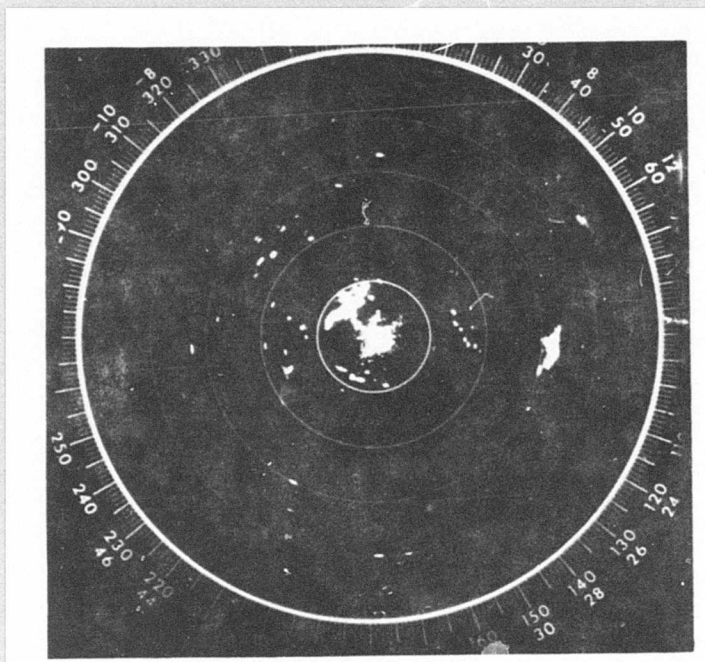


Figure 6. WSR-57 PPI at 0822Z, 22 Dec 1973. Radar settings are identical to those noted in Figure 5. The line of showers is about 30-35 km northwest of Kwajalein, having just passed through the target area. The showers are beginning to dissipate at this time

with the persistence of the WB-57F contrails. The NWS surface observation at Kwajalein at impact time was 2/10 coverage of scattered cumulus clouds at 400 m (1400 ft) and less than 1/10 coverage stratocumulus clouds at 1.5 km (5 kft).

At reentry time the moon was below the horizon and many stars were visible. These stars were sharp, indicating an absence of all clouds with the possible exception of very thin cirrus clouds. Some areas of the sky appeared void of stars; as the RV's penetrated the atmosphere and lit up the sky, the starless areas were seen to be low-level cumulus clouds. One photograph from the TRAP aircraft indicated that one of the RV's passed through a high thin cirrus cloud. Study of other TRAP photographs and observations from the surface showed that this cloud was not on the RV trajectory but that it was at a height greater than 9 km, somewhere between the aircraft and the RV.

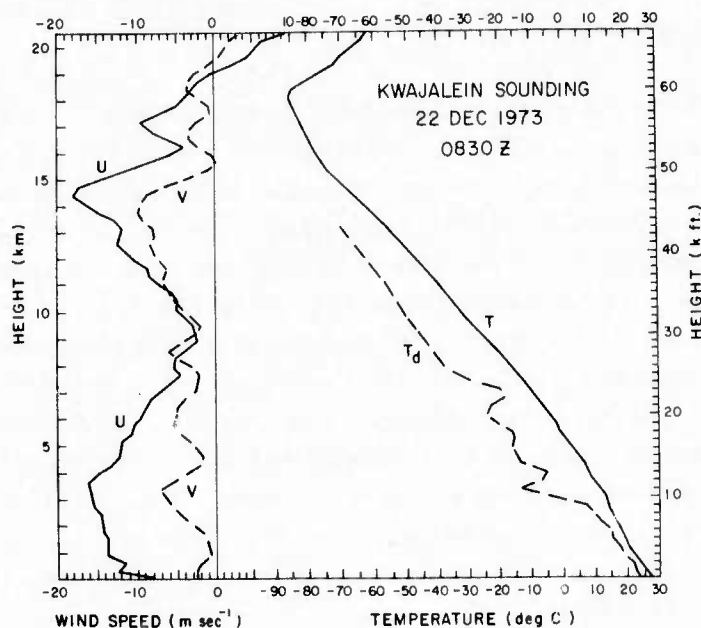


Figure 7a. Sounding from Kwajalein at 0830Z, 22 Dec 1973. Wind components are plotted toward the east (U) and toward the north (V). Winds are from the northeast quadrant at all levels below the tropopause, which is about 18 km, with maximum speed  $20 \text{ m sec}^{-1}$  at 14 km. Significant humidity ( $\text{RH} > 50\%$ ) occurs below 2.7 km, although there are layers with RH near 40% at 4.1 km and about 6.5 km

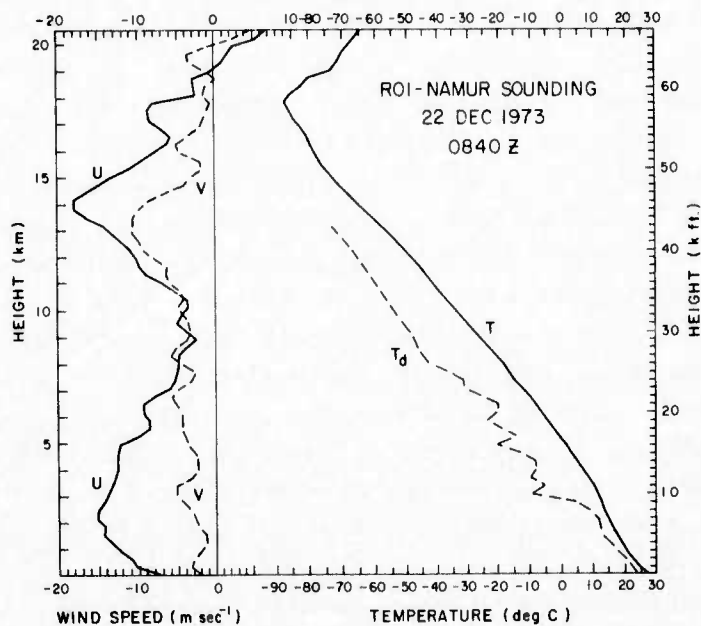


Figure 7b. Sounding from Roi-Namur at 0840Z, 22 Dec 1973. See legend for Figure 7a



### 3. WB-57F WEATHER OBSERVATIONS

Two WB-57F aircraft were at Kwajalein during the period 12-22 December 1973. The operations during that time are summarized in Table 2. Flights prior to launch day were performed for purposes of instrumentation and communications testing, vectoring practice, and cloud sampling. Several specific instrumentation problems encountered during the PVM-3 field operations had been corrected. Details of the objectives and accomplishments of these flights have been provided by MRI.<sup>3</sup> Cloud data were recorded in conjunction with ALCOR weather scans on two days, one prior to the mission day for practice, and on the mission day about 2 to 5 hr before reentry. The weather on these days was insufficient for effective correlation of the radar and aircraft measurements. The operations on 18 and 19 December in conjunction with the TTR-4 radar were feasibility tests of the link-offset mode, which was subsequently implemented at KREMS for the PVM-5 weather documentation in April 1974. Participation of the TTR-4 in these tests was coordinated by AFCRL.

Cloud physics instrumentation was housed in two removable pods mounted near the outer end of each wing, as shown in Figures 8 and 9. These are described in detail by Jahnsen and Heymsfield.<sup>3</sup> The principal instruments were the PMS probes, which measured particle sizes in the ranges 1 to 31  $\mu$  (axially scattering spectrometer), 28 to 310  $\mu$  (optical array cloud particle spectrometer), and 164 to 2170  $\mu$  (optical array precipitation spectrometer). A Formvar particle replicator (MRI Model 1203B) provided a continuous record of the types of hydrometeors encountered by the aircraft. Images of particles greater than 2  $\mu$  in length were preserved in an adhesive resin applied to a 16-mm sampling tape. These data are essential to the analysis of the PMS data, as the computation of ice water content and reflectivity from the one-dimensional size spectra requires an approximation of the crystal habit. A second hydrometeor sampler (MRI Model 1220 foil impactor) recorded images of particles greater than 250  $\mu$  in size on a thin metallic film. Additional instrumentation measured temperature, pressure altitude, and indicated airspeed, which were recorded along with observations by the crew. MRI was responsible for the aircraft instrumentation in general, and EG&G operated the on-board tape recorders.

The WB-57F's were equipped with forward- and downward-looking cameras which were used to supplement the other sensors. The downward-looking F415P camera was used only during the pre-impact, high-altitude photo-mapping run, as described in Section 2.

MRI computed water content  $M$  and radar reflectivity factor  $Z$  from the particle size spectra. Ice crystal sizes measured by the spectrometers are converted to equivalent melted diameters by a calibration equation appropriate to the

Table 2. WB-57F Operations at Kwajalein, December 1973

Date (1973)	Time (GMT)	Pressure (k ft)	Altitude (km)	Remarks
13 Dec		60.0	18.3	Ascent and photo-mapping run over corridor
		49.0	14.9	} Cloud sampling with MPS-36 and ALCOR
		42.0	12.8	
		26.5	8.1	
		13.2	4.0	
15 Dec		38.4	11.7	} Cloud sampling in Kwajalein area
		37.3	11.4	
		34.5	10.5	
		45.0	13.7	Photo-mapping run over atoll
18 Dec	0150-0152	55.0	16.8	} Cloud sampling 350 km SW of Kwajalein
	0235-0237	38.8	11.8	
	0240-0246	32.0	9.8	
	0249-0253	38.5	11.7	
	0257-0303	35.4	10.8	
	0303-0308	39.3	12.0	} Cloud sampling during ascent
	0313-0320	36.3-39	11.1-11.9	
	0322-0329	39.3-42	12.0-12.8	
	0331-0332	35.3-39.2	10.8-11.9	} Vectoring with MPS-36 and TTR-4 in link-offset mode
		54.0	16.5	
		45.0	13.7	
19 Dec	0230-0235	45.0	13.7	} Vectoring with MPS-36 and TTR-4 in link-offset mode
		35.0	10.7	
	0230-0235	45.9	14.0	} Cloud sampling 350 km S of Kwajalein
	0239-0245	43.9	13.4	
	0247-0253	41.9	12.8	
	0257-0300	39.9	12.2	
	0302-0308	38.5	11.7	
	0310-0316	38.0-46.5	11.6-14.2	Cloud sampling during ascent
	0340-0344	44.2	13.5	} Cloud sampling
	0353-0359	42.7	13.0	
	0404-0407	43.2	13.2	
21 Dec		60.0	18.3	Ascent and photo-mapping run over corridor
	0407-0410	38.6	11.8	} Cloud sampling in Kwajalein area
	0414-0417	36.5	11.1	
	0418-1423	34.6	10.5	
	0425-0429	32.7	10.0	
	0430-0436	30.6	9.3	
	0438-0442	28.7	8.7	
	0444-0452	35.3	10.8	
	0453-0503	34.5	10.5	
	0503-0505	34.0	10.4	} Cloud sampling during ascent
	0508-0511	29.1-32.4	8.9- 9.9	
	0513-0517	32.8-35.3	10.0-10.8	
22 Dec	0406-0413	50.0-55.0	15.2-16.8	Cloud sampling during initial climb
	0443-0445	60.0	18.3	Photo-mapping run over corridor
	0505-0510	56.0	17.1	} Cloud sampling with MPS-36, ALCOR, and lidar
	0519-0524	53.0	16.2	
	0533-0539	38.0	11.6	
	0554-0601	24.0	7.3	

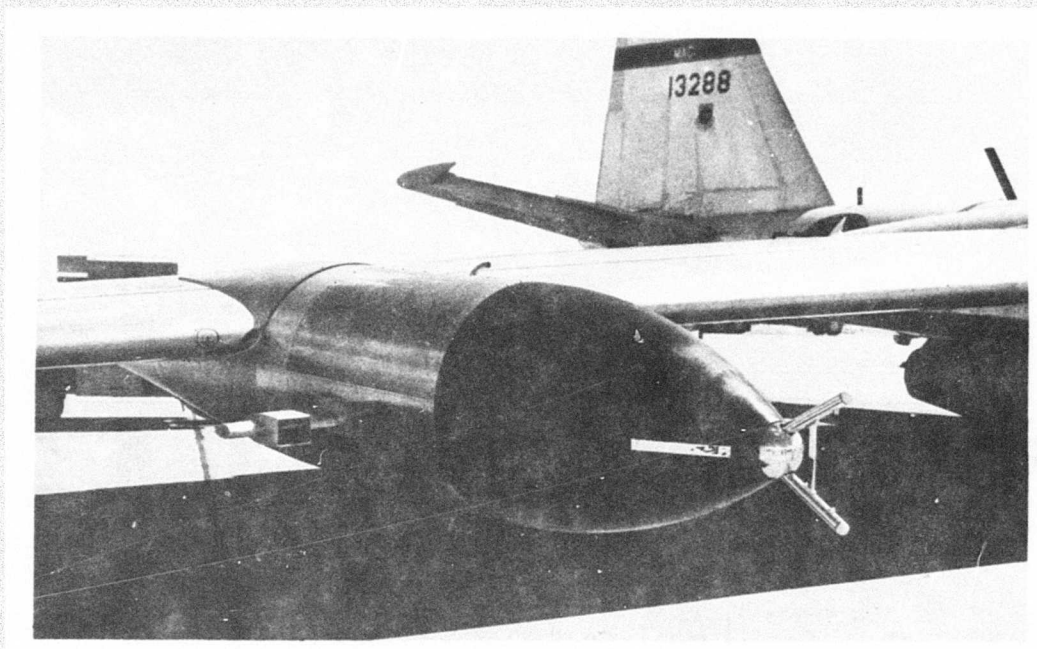


Figure 8. Instrumentation Pod on Right Wing of WB-57F Aircraft. Precipitation spectrometer is at the forward end of the pod, and MRI replicator is on the side

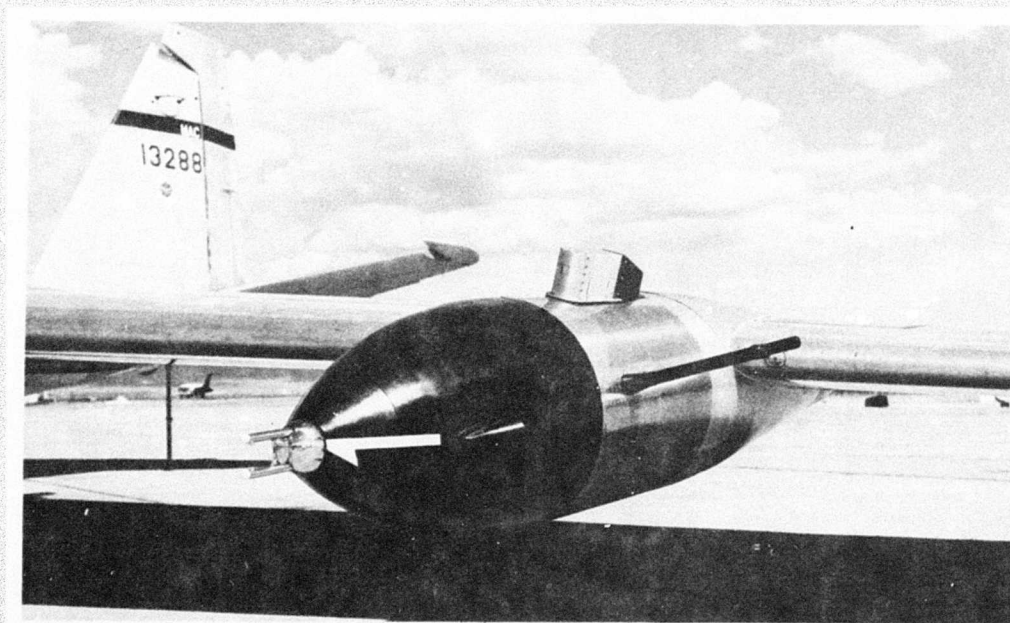


Figure 9. Instrumentation Pod on Left Wing of WB-57F Aircraft. Cloud particle spectrometer is at the forward end, axially scattering spectrometer is on the side, and MRI foil sampler is on the top



type of crystal, as determined from the replicator tape. The water content is proportional to the third moment of the particle size spectrum, or the volume. The radar reflectivity factor is equal to the sixth moment of the size spectrum. These values of Z may be compared with those measured by radar as a check on the validity of the aircraft data reduction. They may also be used with the computed values of M to obtain estimates of Z-M correlations on days when radar data are not available (see Figure 12).

The aircraft flight patterns on STM-8W mission day are shown in Figure 10. The entire operation was conducted prior to launch because of the requirement that the aircraft be on the ground before sunset. An ascent was made in the re-entry corridor about 0350-0405Z to obtain a qualitative profile of the clouds. There was a very thin cirrus deck located about 35 to 40 km due east of Kwajalein at about 8 km altitude. Another patch was estimated to be at a height of 3.5 km. There were scattered thunderstorms in the area. From about 0406-0413Z the aircraft sampled during its initial climb. Particle counts were recorded only on the smallest channels of the scattering probe and the cloud probe. A malfunction of the cloud probe makes its data questionable, but the absence of counts on the precipitation probe and on the upper channels of the scattering probe indicates that the air was essentially clear, with  $M < 10^{-5} \text{ gm m}^{-3}$ .

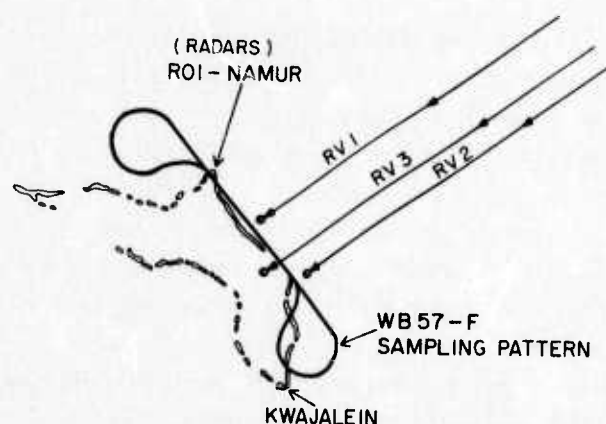


Figure 10. Flight Pattern for WB-57F Cloud Sampling. Photo-mapping pass is along the re-entry trajectories. Weather sampling in conjunction with ALCOR is along a radial from Roi-Namur toward Gellinam

Following the photo-mapping runs, cloud sampling runs were made at four different altitudes. Figure 11 shows the aircraft position measured by the



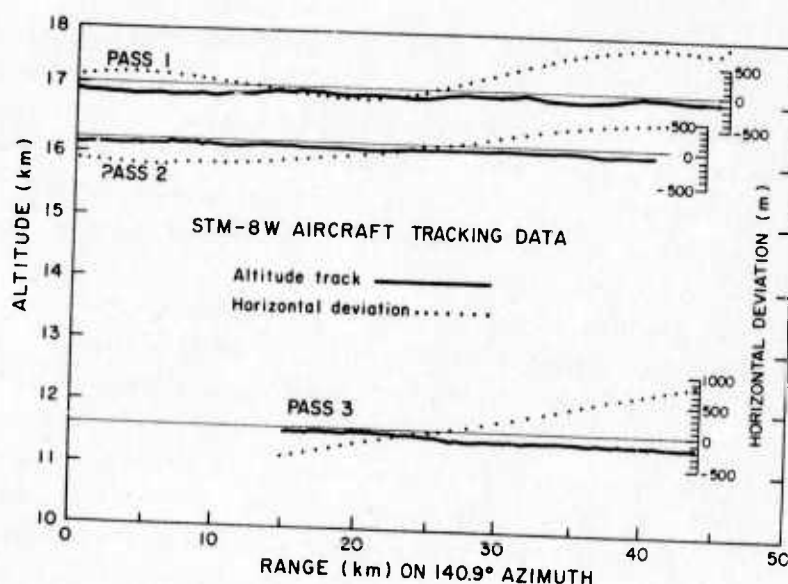


Figure 11. Deviations of the WB-57F Aircraft From Nominal Flight Paths. MPS-36 tracking data show that the aircraft is uniformly low by 100-200 m relative to the nominal altitudes. Horizontal deviation is displayed as positive to the east of the nominal azimuth. Data for Pass 4 at 7.3 km and part of Pass 3 are not available

MPS-36 tracking radar during the sampling runs, relative to the nominal flight paths. Particle counts were recorded only on the smallest size channels of the scattering probe for most of the duration of these runs, yielding estimates of ice water content less than  $10^{-5} \text{ gm m}^{-3}$ . On the fourth pass a few counts were recorded on the precipitation probe during a 1-sec interval, with  $M \approx 2.2 \times 10^{-4} \text{ gm m}^{-3}$ . High-level cirrus clouds, near the tropopause, were visible to the west and south of the corridor during the cloud sampling operations. Because of the northeasterly winds, these were not in the corridor at reentry time, as confirmed by the lidar observations.

Correlations of  $M$  and  $Z$  computed from the PMS data were not made for STM-8W mission day due to the lack of significant weather. Correlations using PMS data were made for other days in an attempt to document the variability of the  $Z$ - $M$  relations from day to day in the Kwajalein area. Some results of this analysis are shown in Figure 12. The clouds on 19 December were composed of small crystals and appeared translucent to the aircrew and surface observers despite values of  $M$  up to  $10^{-2} \text{ gm m}^{-3}$ . On 21 December the clouds were composed principally of large crystals, appearing more dense and yielding higher values of  $Z$  for given values of  $M$ , although the values of  $M$  were not much

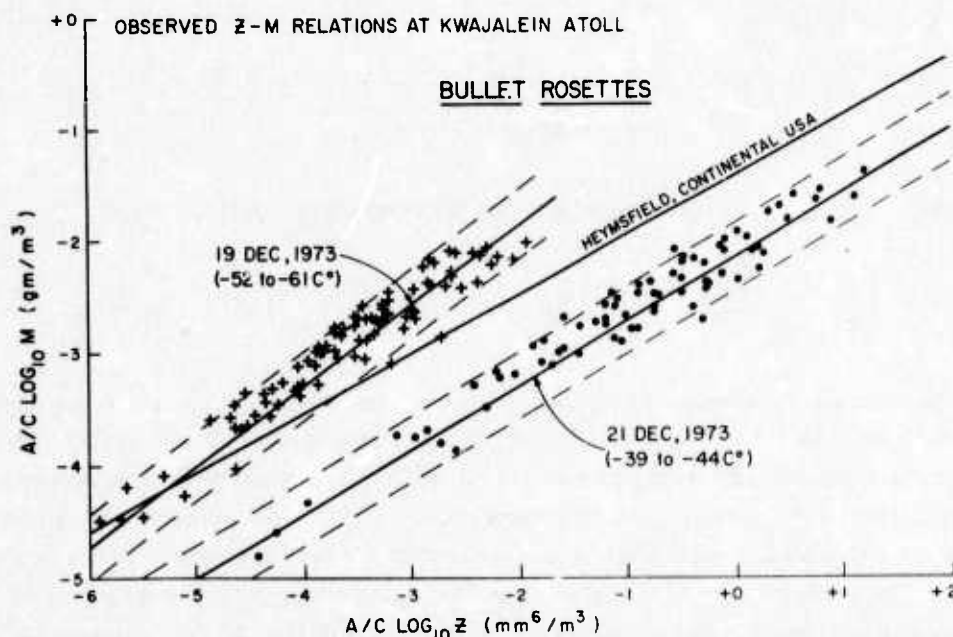


Figure 12. Correlations of Z and M Derived From WB-57F Data at Kwajalein. These show the differences resulting from variations in the crystal size spectrum. Flights were at 13 km on 19 December and 11 km on 21 December. Z-M equation for continental U.S. cirrus is shown for comparison

greater than on 19 December. These large crystals were responsible for the solar halo and parhelia (sun dogs) observed from the surface. A Z-M equation derived by Heymsfield<sup>5</sup> from PMS data taken in high-altitude cirrus clouds over Colorado is shown in Figure 12 for comparison. We used this equation for deriving preliminary estimates of water content from the radar weather data. Figure 12 implies that these estimates are accurate to somewhat better than an order of magnitude.

#### 4. ALCOR WEATHER OBSERVATIONS

Weather data were recorded by ALCOR in conjunction with the WB-57F cloud sampling operations described in Section 3. Weather scans were also made along the trajectories immediately before and after the reentry. The complete ALCOR mission weather support is presented in Table 3.

The reflectivity factor  $Z$  ( $\text{mm}^6 \text{m}^{-3}$ ) was computed by the equation

5. Heymsfield, A. J. (1973) The Cirrus Uncinus Generating Cell and the Evolution of Cirriform Clouds, PhD thesis, The Univ. of Chicago.

$$Z = C\sigma/r^2 \quad (1)$$

or

$$\text{dBZ} = 10 \log C + 10 \log \sigma - 20 \log r \quad (2)$$

where  $\sigma$  is the cross-section ( $\text{m}^2$ ),  $r$  is the range (km), and

$$C = \frac{\lambda^4 \times 10^{10}}{\pi^5 \times |K|^2} \left[ \frac{8 \ln 2}{\pi \theta^2 h \times 10^6} \right], \quad (3)$$

where  $\lambda$  is the wavelength (5.30 cm),  $h$  is the pulse length (37.5 m),  $\theta$  the beam-width ( $5.24 \times 10^{-3}$  rad), and  $|K|^2 = 0.197$  for radar backscatter from ice crystals, and 0.93 for backscatter from rain. Because ALCOR transmits a frequency-modulated "chirp" pulse, the pulse length used in the above computation is not a physical pulse length but rather a compressed pulse length corresponding to the output of a pulse compression network in the radar receiver. Comparisons of chirp and constant-frequency radar weather data from the TTR-4 radar at Kwajalein<sup>6</sup> showed that the computational factor determined from Eq. (3) above had to be increased by 3 dB for the chirp data. Thus  $10 \log C = 86.5$  for the ALCOR observations above the freezing level, and 79.8 in rain.

Table 3. ALCOR Weather Support for STM-8W, 22 Dec 1973

Aircraft Correlations		Trajectory Scans	
Time (GMT)	Altitude (km)	Time (GMT)	Trajectory
0505:16	17.1	0828:05-0829:03	RV1 (pre-impact)
0507:16	17.1		
		0834:39-0835:19	RV1
0519:27	16.2	0835:36-0836:05	RV2
0521:27	16.2	0836:19-0836:42	RV3
		0836:58-0837:30	Vertical
0532:37	11.6		
0534:37	11.6	0838:15-0838:55	RV1
		0839:10-0839:39	RV2
0553:03	7.3	0839:53-0840:16	RV3
0557:35	7.3	0840:32-0841:04	Vertical
		0841:51-0842:31	RV1
		0842:45-0843:14	RV2
		0843:29-0843:52	RV3
		0844:08-0844:39	Vertical

6. Metcalf, J.I., Barnes, A.A., Jr., and Nelson, L.D. (1975a) Water content and reflectivity measurements by "chirp" radar, 16th Radar Meteor. Conf., Am. Meteor. Soc., 492-495.

The radar data were handled as shown in Figure 13. We first surveyed the films of the radar RTI intensity-modulated display to determine the time intervals of interest; that is, the times when weather echoes were observed. Lincoln Laboratory computed the reflectivity according to Eq. (2) and provided to AFCRL tabulated values of reflectivity and radar cross-section averaged over a specified number of range gates within the 2.5-km data window and over a specified number of pulses. None of the scans taken in conjunction with the WB-57F sampling were reduced, as no weather echoes were observed at these altitudes at these times. The data for the trajectory scans were averaged over 11 gates, giving 160-m beamwise resolution, and 20 pulses, giving 90-m vertical resolution or better. The reflectivity values were hand-plotted onto a range-height array for subsequent analysis. Only the signal values from the left circular polarization (opposite to the transmitted polarization) were used for this analysis, as these are 15 to 20 dB greater than those received on right circular polarization for weather echoes.

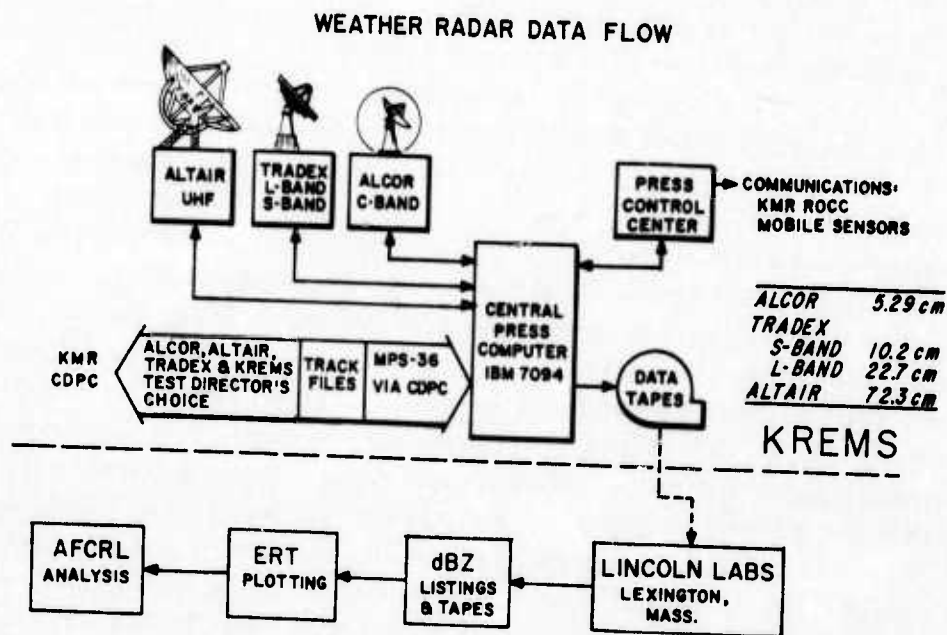


Figure 13. Radar Weather Data Flow Diagram. ALCOR is the principal weather sensor, with TRADEX S-band as backup. Hand plotting of data listings provided by Lincoln Laboratory is accomplished by Environmental Research and Technology, Inc., on contract by AFCRL

The quantity  $Z$  is the factor of the received signal power which is dependent only on meteorological parameters. It is equal to the sixth moment of the particle



size spectrum, and thus is not a direct measure of the water content which is proportional to the third moment, that is, the volume. The relation of reflectivity to water content depends on the spectrum of ice crystals or water drops in a cloud. For interpretation of the radar data in the absence of good correlation measurements by radar and aircraft, we used a Z-M equation appropriate to ice crystals:

$$M = 0.038 Z^{0.529}, \quad (4)$$

above the freezing level.<sup>5</sup> Below the freezing level we used a Z-M equation appropriate to tropical rain:

$$M = 0.011 Z^{0.43}, \quad (5)$$

derived from equations presented by Battan.<sup>7</sup> (It should be noted that this Z-M equation was derived from surface observations and is therefore not strictly applicable to observations in clouds; however, it is useful for order-of-magnitude estimates of the cloud water content.)

An RHI scope had been installed at KREMS prior to the STM-8W mission. This SPA-40 scope had been found by AFCRL as surplus equipment and transferred to Lincoln Laboratory. The RHI display provided more effective weather reconnaissance data than the A-scope display used for the PVM-3 operations. Photographs of the RHI scope, such as those in Figure 14, were used to obtain heights of cloud layers for the aircraft sampling. In addition to this function, the RHI scope permitted general surveillance of the reentry corridor weather. The earliest RHI photographs on the mission day revealed a very weak layer near 8.8 km, which had disappeared by the time of the aircraft sampling operations. This layer evidently persisted to the time of reentry, however, as an echo was observed at this altitude on the RV1 trajectory scans. Other layers were observed on the RHI display at 7 km, 5 km, 4.5 km, and below 3 km. The layer near 7 km was no longer detectable by the time of the aircraft sampling pass at this altitude. The thinness of these layers and the absence of visible clouds at these altitudes during the aircraft sampling operations suggests that they were due to backscatter from refractive index fluctuations in the clear atmosphere. This hypothesis is supported further by the sharp fluctuations in the humidity sounding (Figure 7) between 3 and 7 km in conjunction with the relatively large wind shear at these altitudes.

A weather scan was made along the RV1 trajectory just prior to reentry. Following vehicle impact, a sequence of scans was made, once down each trajectory

7. Battan, L. J. (1973) Radar Observations of the Atmosphere, Univ. of Chicago Press, 324 pp.

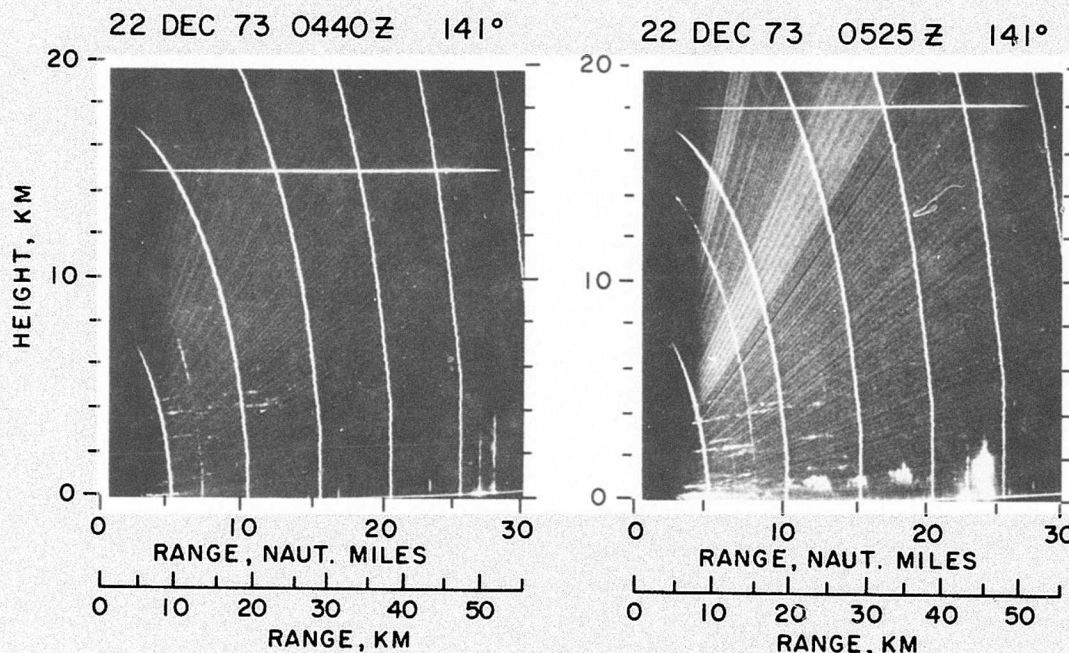


Figure 14. ALCOR RHI Scans During Pre-Mission Aircraft Operations. Range markers are at intervals of 9.3 km (5 n.m.) and height marker (horizontal line) is at 15.2 km (50 kft) and 18.3 km (60 kft) in the respective scans. Very weak echo layers can be seen near 9 km at 0440Z and near 6.5 km at 0525Z. These and the multiple layers below 5 km are thought to be due to fluctuations of the refractive index in clear air, as no clouds were observed at these altitudes. The cellular echoes below 1.5 km are due to low-level cumulus clouds

from 23 km to 0.5 km, and once vertically over the radar, and repeated three times. The sequential scans on each trajectory provided a time history of the weather on the trajectory. The vertical scans were intended to reveal high thin layers which might be too weak to appear in the trajectory scans, since the minimum detectable signal level increases as the square of the slant range.

Two of the scans of the RV1 trajectory are shown in Figure 15. (Data from the first post-impact scan of the RV1 trajectory were not recorded.) In addition to the echoes below 6 km, these trajectory scans revealed a weak echo near 8.5 km. This echo was about 3 dB above the minimum detectable signal, implying an ice water content about  $2.6 \times 10^{-3} \text{ gm m}^{-3}$ . The thickness of the layer was less than 300 m. The echoes near 5.5 km implied an ice water content about  $1.8 \times 10^{-3} \text{ gm m}^{-3}$ . The lower echoes on the pre-impact scan implied water content (liquid) about  $6 \times 10^{-4} \text{ gm m}^{-3}$  at 3.2 km, and  $1.7 \times 10^{-3} \text{ gm m}^{-3}$  at 1.5 km. The low-altitude echoes on the second post-impact scan corresponded to water content about  $1.7 \times 10^{-3} \text{ gm m}^{-3}$ , and  $4.5 \times 10^{-3} \text{ gm m}^{-3}$  at 2.5 km and 1.6 km, respectively.

The first two post-impact scans of the RV2 trajectory are shown in Figure 16. The echoes above 4 km and probably the echo at 2.8 km were due to pieces of



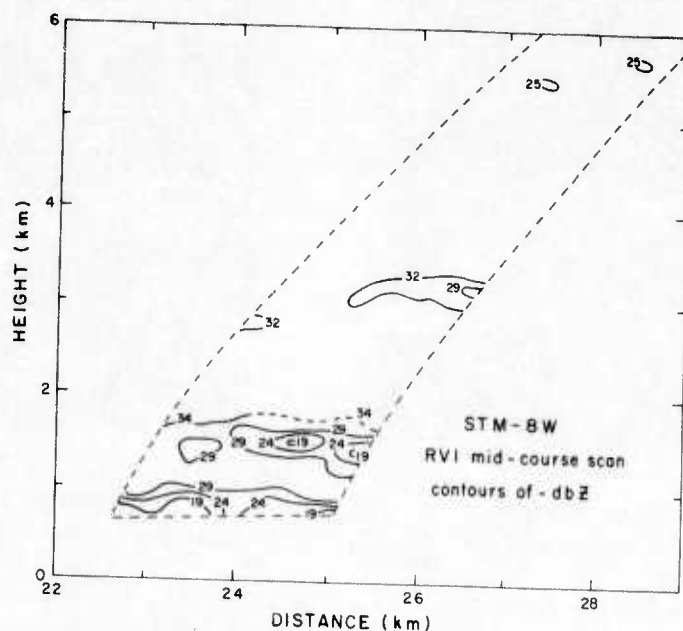


Figure 15a. ALCOR Scan of STM-8W RV1 Trajectory at 0828Z, 22 Dec 73. Contours are of  $-10 \log Z$ , with  $Z$  in  $\text{mm}^6 \text{m}^{-3}$ . Contours at 5.5 km show maximum  $Z$  values of a layer just above the threshold of detectability. Water content of all the observed layers is less than  $0.003 \text{ gm m}^{-3}$

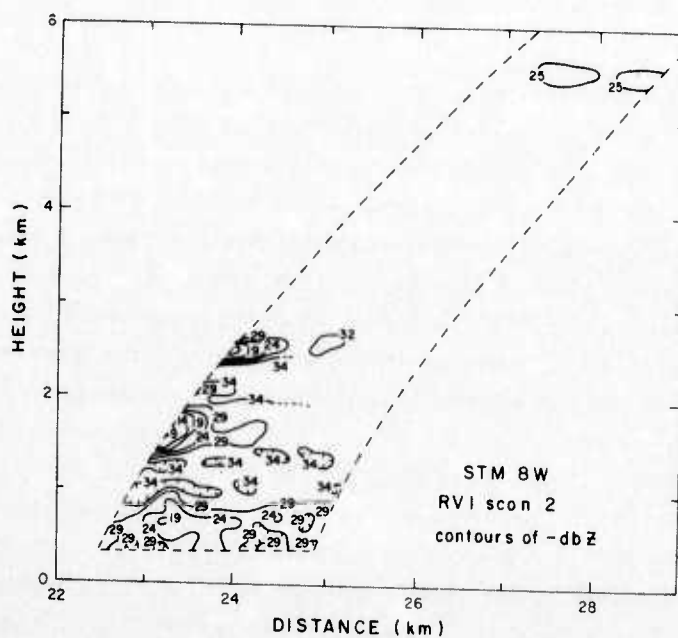


Figure 15b. ALCOR Scan of STM-8W RV1 Trajectory at 0838Z, 22 Dec 73. Contours are of  $-10 \log Z$ , with  $Z$  in  $\text{mm}^6 \text{m}^{-3}$ . Layer at 5.5 km persists, although structure below 3.5 km has changed markedly



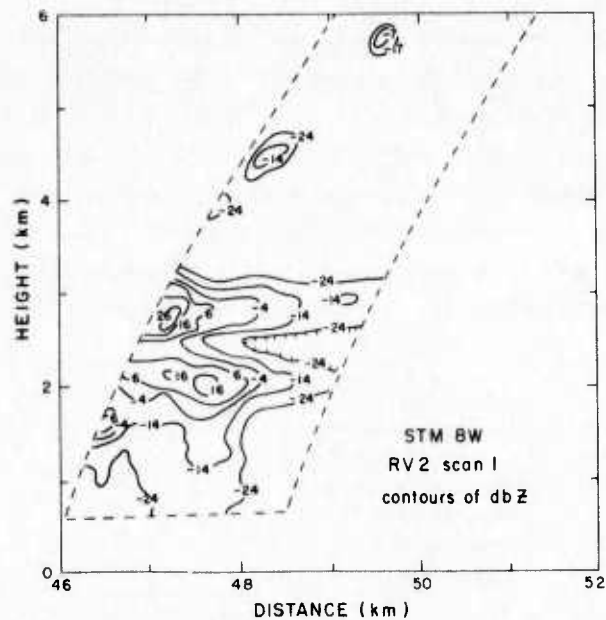


Figure 16a. ALCOR Scan of STM-8W RV2 Trajectory at 0836Z, 22 Dec 73. Contours are of  $10 \log Z$ , with  $Z$  in  $\text{mm}^6 \text{m}^{-3}$ . Echoes at 5.8km, 4.5km, and 2.8km are thought to be due to debris, as they have characteristics of solid targets. The maximum water content at 2.0km is approximately  $0.07 \text{ gm m}^{-3}$ .

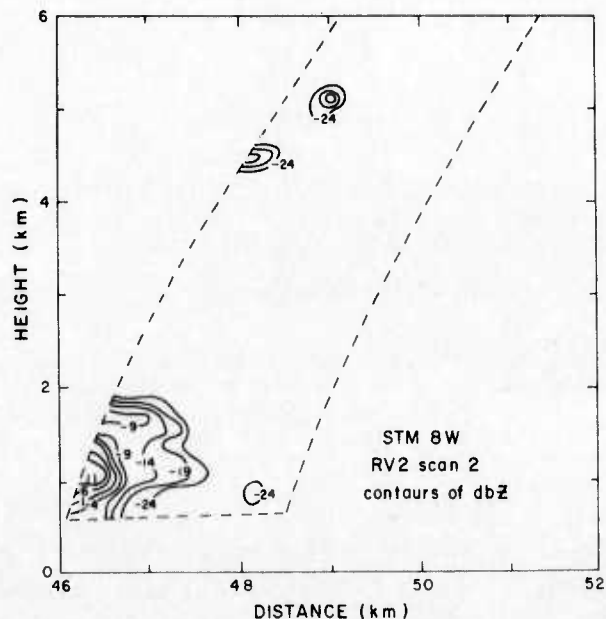


Figure 16b. ALCOR Scan of STM-8W RV2 Trajectory at 0839Z, 22 Dec 73. Contours are of  $10 \log Z$ , with  $Z$  in  $\text{mm}^6 \text{m}^{-3}$ . Echoes at 5.1 km and 4.5 km are due to debris. Cloud below 2 km has maximum water content of approximately  $0.05 \text{ gm m}^{-3}$ .

debris, since the received signals on both polarizations were nearly equal. The echo structure below 2 km had the character of a weather echo, and implied a maximum water content about  $0.07 \text{ gm m}^{-3}$  at 2 km on the first scan and  $0.05 \text{ gm m}^{-3}$  at 1 km on the second scan. No weather echoes were observed on any of the RV3 trajectory scans. The approximate minimum detectable ice water content on the three trajectories is shown in Figure 17. The weak layer detected near 8.5 km on the RV1 trajectory was below the minimum detectable level on the other trajectories, which were further from the radar.

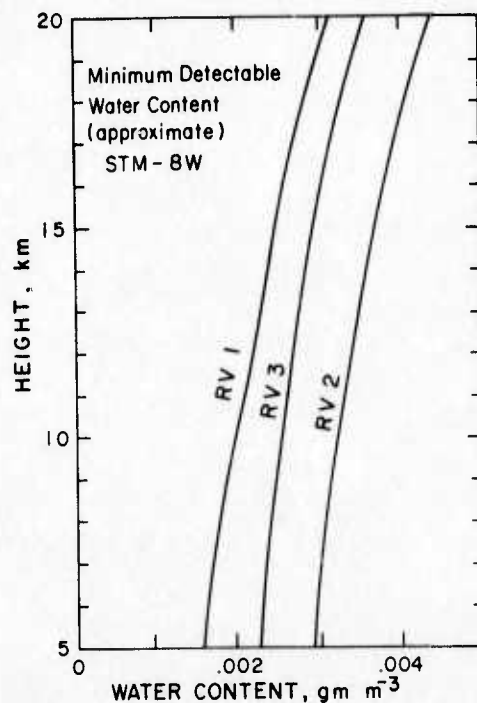


Figure 17. Approximate Minimum Detectable Ice Water Content on STM-8W Trajectories. Any high clouds which might be present must be less dense than these values

The first vertical scan, shown in Figure 18, revealed several echoes which were not observed on the trajectories. The 8 to 8.5 km layer had ice water content about  $9 \times 10^{-4} \text{ gm m}^{-3}$ , much below the minimum detectable levels on the trajectories. However, its appearance on the vertical scan as well as on the closest trajectory scan suggests strongly that it covered a wide area, including all the trajectories.

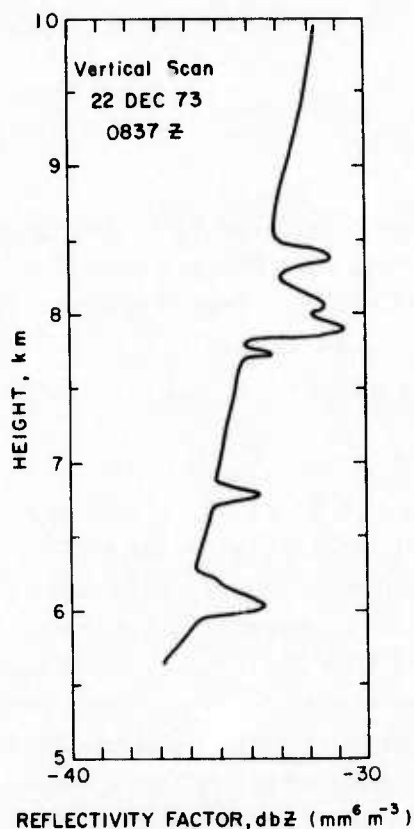


Figure 18. Reflectivity Profile Observed on ALCOR Vertical Scan at 0837Z, 22 Dec 73. Reflectivity of -31 dBZ at 8 km corresponds to ice water content of approximately  $9 \times 10^{-4} \text{ gm m}^{-3}$

## 5. SUMMARY AND CONCLUSIONS

The weather criterion for the STM-8W reentry was satisfied. A thin cloud layer, observed by radar about 8.5 km on the RV1 trajectory and on the vertical scans, probably extended across all the trajectories. Its ice water content was about  $0.003 \text{ gm m}^{-3}$  on the RV1 trajectory, and less than  $0.003 \text{ gm m}^{-3}$  on the other trajectories. Absence of this layer in the lidar observations, which might be due in part to its spatial variability, suggests that its ice water content might be less than  $10^{-4} \text{ gm m}^{-3}$ . It did not impair optical tracking of the reentry vehicles. Low clouds were detected on the RV1 and RV2 trajectories, indicative of the 2/10 coverage of low cumulus clouds at the time of reentry reported by the NWS.

The weather severity index used as a launch criterion for later tests in this series is defined by

$$WSI = \int_{h_1}^{h_2} M h dh, \quad (6)$$

where  $h_1$  is normally equal to zero and  $h_2$  is the height (km) of the highest cloud top on the trajectory. (The units of WSI are  $gm\ km^2\ m^{-3}$ .) In the present case where the weather consists mainly of a few thin layers, this may be approximated by a summation over all the cloud layers:

$$WSI \approx \sum_i M_i \bar{h}_i \Delta h_i. \quad (7)$$

The WSI based on the observed clouds was about 0.01 for RV1 and 0.1 for RV<sub>2</sub> (due to the low-level cloud), and less than 0.1 for RV3.

Aircraft observations prior to launch revealed thin cirrus clouds near the tropopause (18 km) to the west and south of the reentry area. Patches of cloud were also observed about 3.5 km and 8 km altitude about 3 to 4 hr before launch. Very few particle counts were recorded on the PMS instruments during the cloud sampling operations, and no radar weather echoes were detected at the sampling altitudes. A line of showers passed through the target area about 15 min before reentry, with tops about 6 to 7 km. These may have been the source of the cloud layers observed on the ALCOR trajectory weather scans taken immediately after impact.

Improvements in the operational procedures were based on experience gained during the PVM-3 mission support in August 1973. The WB-57F instrument pods had been shielded to eliminate interference from ALCOR, which had been noted in the August 1973 data. An RHI display had been installed at the PRESS Control Center to facilitate the work of the radar meteorologists there. Correlation of aircraft and radar weather data, already shown to be difficult by the PVM-3 experience, was again unnecessary due to the absence of significant weather. However, preliminary tests of the link-offset mode showed this to be the most promising technique for obtaining the correlation weather data for future missions.



## References

1. Metcalf, J. I., Barnes, A. A., Jr., and Kraus, M. J. (1975b) Final Report of PVM-4 and PVM-3 Weather Documentation, AFCRL-TR-75-0097, Air Force Cambridge Research Laboratories, Hanscom AFB, MA.
2. Wilmot, R. A., Cisneros, C. E., and Guiberson, F. L. (1974) High cloud measurements applicable to ballistic missile systems testing, 6th Conf. Aerosp. and Aeronaut. Meteor., Am. Meteor. Soc., 194-199.
3. Jahnsen, L. J., and Heymsfield, A. J. (1974) STM-8W Mission WB-57F Instrumentation and Cloud Particle Measurements, MRI 74 FR-1189, Meteorology Research, Inc., Altadena, CA.
4. Uthe, E. E., Allen, R. J., and Russell, P. B. (1974) Light Detection and Ranging (LIDAR) Support for STM-8W and PVM-5 Reentry Operations, SRI Project 2859, Stanford Research Institute, Menlo Park, CA.
5. Heymsfield, A. J. (1973) The Cirrus Uncinus Generating Cell and the Evolution of Cirriform Clouds, PhD thesis, The Univ. of Chicago.
6. Metcalf, J. I., Barnes, A. A., Jr., and Nelson, L. D. (1975a) Water content and reflectivity measurements by "chirp" radar, 16th Radar Meteor. Conf., Am. Meteor. Soc., 492-495.
7. Battan, L. J. (1973) Radar Observations of the Atmosphere, Univ. of Chicago Press, 324 pp.

## Symbols

AFCRL	Air Force Cambridge Research Laboratories
ALCOR	ARPA-Lincoln C-band Observables Radar
ARPA	Advanced Research Projects Agency
CDPC	Central Data Processing Computer
DAPP	Data Acquisition and Processing Program
DMSP	Defense Meteorological Satellite Program
EG&G	Edgerton, Germeshausen, and Grier, Inc.
ERT	Environmental Research and Technology, Inc.
GMT	Greenwich Mean Time
KMR	Kwajalein Missile Range
KREMS	Kiernan Reentry Measurements Site
LIDAR	Light Detection and Ranging (optical analog of RADAR)
M	Water content (liquid or ice), $\text{gm m}^{-3}$
MRI	Meteorology Research, Inc.
NWS	National Weather Service
PMS	Particle Measuring Systems, Inc.
PPI	Plan Position Indicator
PRESS	Pacific Range Electromagnetic Signature Studies
PVM	Production Verification Missile
RHI	Range Height Indicator
ROCC	Range Operations Control Center
RTI	Range Time Intensity
RV	Reentry Vehicle

## Symbols

SAMSO	Space and Missile Systems Organization
SAMTEC	Space and Missile Test Center
SRI	Stanford Research Institute
STM	Special Test Missile
TRADEX	Target Resolution and Discrimination Experiment
TRAP	Terminal Radiation Program
TTR	Target Tracking Radar
WSI	Weather Severity Index
Z	Radar Reflectivity Factor, $\text{mm}^6 \text{m}^{-3}$
Z	Greenwich Mean Time

Printed by  
United States Air Force  
Hanscom AFB, Mass. 01731